

Short summary

Yann-Edwin Keta

November 12th, 2019

1 Model

We consider an ensemble of N spherical ABPs i , with positions \underline{r}_i and orientations θ_i , which are self-propelled along the direction $\underline{u}_i \equiv (\cos(\theta_i), \sin(\theta_i))$. We have the following dimensionless equations of motion [1],

$$\begin{aligned}\dot{\underline{r}}_i(t) &= \frac{1}{3} \frac{\sigma}{l_p} \tilde{F}_{i,ex}(t) + \underline{u}_i(t) + \sqrt{\frac{2}{3} \frac{\sigma}{l_p}} \underline{\eta}_i(t), \\ \dot{\theta}_i(t) &= \sqrt{2 \frac{\sigma}{l_p}} \xi_i(t),\end{aligned}\tag{1}$$

where $\tilde{F}_{i,ex}$ is the total force applied on particle i deriving from a WCA potential, l_p is the persistence length, σ is the particle diameter, and $\underline{\eta}_i \equiv (\eta_{x,i}, \eta_{y,i})$ and ξ_i are independent Gaussian white noises of unit variance and zero mean.

We define the normalised rate of active work,

$$w(t_0; \tau) = \frac{1}{N\tau} (S) \int_{t_0}^{t_0+\tau} \sum_{i=1}^N \underline{u}_i(t) \cdot d\underline{r}_i(t) = \frac{1}{2N\tau \Delta t} \sum_{t=0}^{\tau-1} \sum_{i=1}^n (\underline{u}(\theta_{i,t_0+t+1}) + \underline{u}(\theta_{i,t_0+t})) \cdot (\underline{r}_{i,t_0+t+1} - \underline{r}_{i,t_0+t}),\tag{2}$$

which we can write as a sum of three terms,

$$\begin{aligned}w_f(t_0; \tau) &= \frac{1}{2N\tau} \sum_{t=0}^{\tau-1} \sum_{i=1}^n (\underline{u}(\theta_{i,t_0+t+1}) + \underline{u}(\theta_{i,t_0+t})) \cdot \frac{1}{3} \frac{\sigma}{l_p} \tilde{F}_{i,ex,t_0+t}, \\ w_\theta(t_0; \tau) &= \frac{1}{2} \left(1 + \frac{1}{N\tau} \sum_{t=0}^{\tau-1} \sum_{i=1}^N \cos(\theta_{i,t_0+t+1} - \theta_{i,t_0+t}) \right), \\ w_\eta(t_0; \tau) &= \frac{1}{2N\tau} \sum_{t=0}^{\tau-1} \sum_{i=1}^N (\underline{u}(\theta_{i,t_0+t+1}) + \underline{u}(\theta_{i,t_0+t})) \cdot \sqrt{\frac{2}{3} \frac{\sigma}{l_p} \frac{1}{\Delta t}} \underline{\eta}_{i,t_0+t+1},\end{aligned}\tag{3}$$

respectively the *force*, *orientation*, and *noise* part of the active work.

We also define an order parameter,

$$\underline{\nu}(t) = \frac{1}{N} \sum_{i=1}^N \underline{u}(\theta_i(t)),\tag{4}$$

with mean and correlations ¹

$$\begin{aligned}\langle \underline{\nu}(t_0) \rangle &= 0, \\ \langle |\underline{\nu}(t_0)| \rangle &= \frac{1}{\sqrt{2N}}, \\ \langle \delta \underline{\nu}(t_0 + \tau) \cdot \delta \underline{\nu}(t_0) \rangle &= \frac{1}{N} \exp\left(-\frac{\sigma}{l_p} \tau\right), \\ \langle \delta |\underline{\nu}|(t_0 + \tau) \delta |\underline{\nu}|(t_0) \rangle &= \frac{1}{4N} \exp\left(-2 \frac{\sigma}{l_p} \tau\right),\end{aligned}\tag{5}$$

in the absence of symmetry breaking.

¹Refer to appendix E of [1] for the derivation of the order parameter norm dynamics which we use to infer the corresponding results of equation 5.

2 One-particle quantities

We check our algorithm and set benchmarks by considering the *free* or *single particle* case, $\tilde{F}_{i,ex} = 0$.

We can analytically derive the mean squared displacement,

$$\langle (\underline{r}(t_0 + \Delta t) - \underline{r}(t_0))^2 \rangle = \frac{l_p}{\sigma} \left(\Delta t + \frac{l_p}{\sigma} \left(\exp \left(-\frac{\sigma}{l_p} \Delta t \right) - 1 \right) \right) + \frac{4}{3} \frac{\sigma}{l_p} \Delta t. \quad (6)$$

and the active work mean and correlations

$$\begin{aligned} \langle w(t_0; \tau) \rangle &= 1, \\ \forall \tau \geq \tau_0, \langle \delta w(t_0; \tau_0) \delta w(t_0; \tau) \rangle &= \frac{2}{3} \frac{\sigma}{l_p} \frac{1}{\tau}, \\ \forall \tau \geq \tau_0, \langle \delta w(t_0; \tau_0) \delta w(t_0 + \tau; \tau_0) \rangle &= 0. \end{aligned} \quad (7)$$

These theoretical predictions match the numerical results.

3 Active work covariances

We argue that

$$\langle \delta w(t_0; \tau_0) \delta w(t_0 + \tau; \tau_0) \rangle \approx \langle \delta w_f(t_0; \tau_0) \delta w_f(t_0 + \tau; \tau_0) \rangle + \langle \delta w_\eta(t_0; \tau_0) \delta w_f(t_0 + \tau; \tau_0) \rangle, \quad (8)$$

since that the fluctuations of the orientation part of the active work are negligible for low integration time steps, and that the orientational and translational noises are independent.

We plot the covariances between the different part of the active work with a delay τ in figure 1.

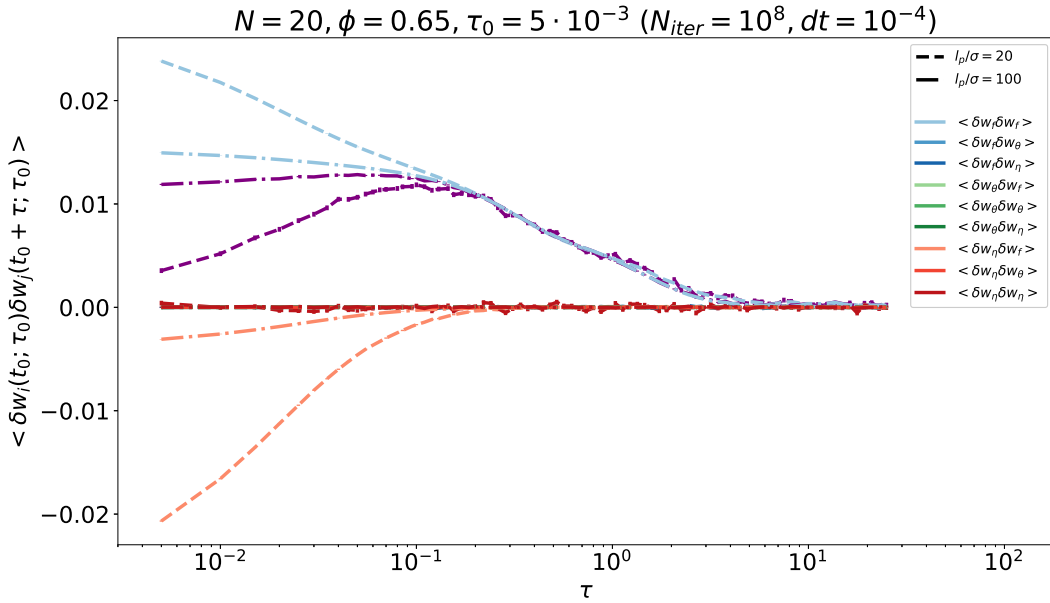


Figure 1: Covariances of active work parts with a delay τ , for $l_p/\sigma = 20$ (dashed lines) and $l_p/\sigma = 100$ (dash-dotted lines). All available intervals but those overlapping with $t_0 \leq 3l_p/\sigma$ were used to compute the means. These curves are qualitatively independent of the choice of τ_0 , this particular choice is a balance between noise reduction and low time resolution. Purple curves correspond to the total active work covariance.

We observe that

- the covariance of the force part of the active work and itself with a delay τ is a positive, monotonically decreasing function of τ , with a length scale which increases with persistence length,
- the covariance of the noise part of the active work and the force part with a delay τ is a negative, monotonically increasing function of τ , with a length scale which is qualitatively independent of the persistence length,
- the covariance of the active work and itself with a delay τ is a non-monotonic function of τ , with a peak at $\tau \approx 10^{-1}$.

3.1 Covariance of noise and force part

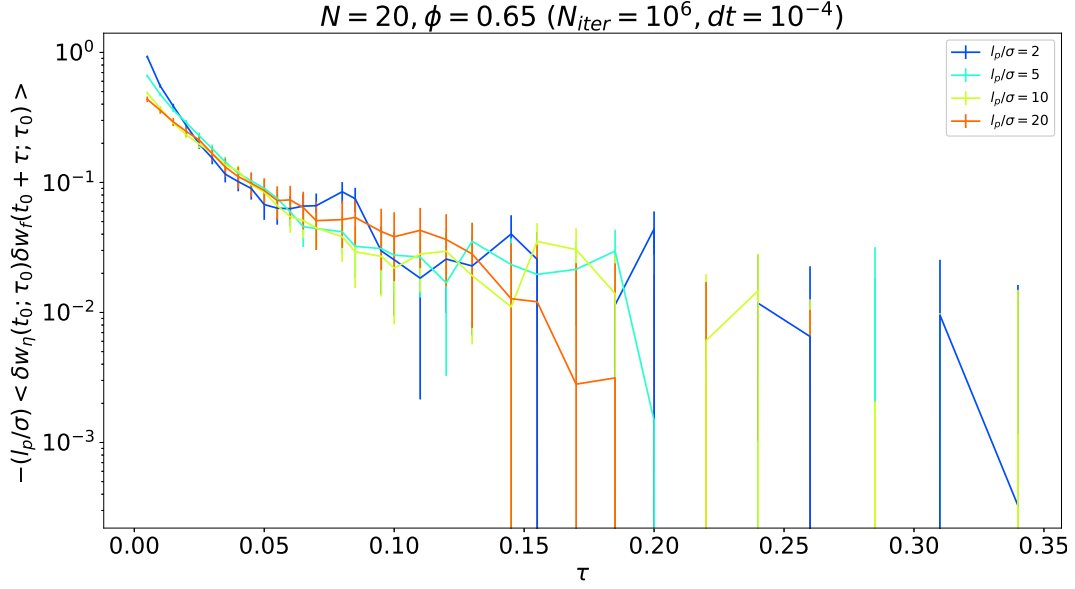


Figure 2: Covariance of the noise part of the active work and the force part with a delay τ .

We have that for the few values of persistence length tested, $2 \leq l_p/\sigma \leq 20$, the time scale of decrease of the absolute value of $\langle \delta w_\eta(t_0; \tau_0) \delta w_f(t_0 + \tau; \tau_0) \rangle$ is qualitatively independent of the persistence length (figure 2).

We argue that this time scale is set by the interaction potential. Consider a single particle in a harmonic potential

$$V(\underline{r}(t)) = \frac{1}{2} k \underline{r}(t)^2.$$

Motivated by figures 1 and 2, we assume that $l_p/\sigma \gg \tau_d$, where τ_d is the relevant time scale of decrease, *i.e.* we can consider that the orientation of the particle is constant. We then have the following equation of motion

$$\dot{\underline{r}}(t) = -\frac{1}{3} \frac{\sigma}{l_p} \nabla V(\underline{r}(t)) + \underline{u}_0 + \sqrt{\frac{2}{3} \frac{\sigma}{l_p}} \underline{\eta}(t). \quad (9)$$

We can write

$$\begin{aligned} d \left\langle \left(\underline{\eta}_i(t_0) \cdot \underline{u}_0 \right) \left(\nabla V(\underline{r}(t_0 + t)) \cdot \underline{u}_0 \right) \right\rangle &= \left\langle \left(\underline{\eta}_i(t_0) \cdot \underline{u}_0 \right) \left(\underbrace{\nabla^2 V(\underline{r}(t_0 + t))}_k d\underline{r}(t_0 + t) \cdot \underline{u}_0 \right) \right\rangle \\ &= -k \frac{1}{3} \frac{\sigma}{l_p} \left\langle \left(\underline{\eta}_i(t_0) \cdot \underline{u}_0 \right) \left(\nabla V(\underline{r}(t_0 + t)) \cdot \underline{u}_0 \right) \right\rangle dt, \end{aligned}$$

such that

$$\left\langle \left(\underline{\eta}_i(t_0) \cdot \underline{u}_0 \right) \left(\nabla V(\underline{r}(t_0 + \tau)) \cdot \underline{u}_0 \right) \right\rangle \propto \exp \left(-k \frac{1}{3} \frac{\sigma}{l_p} \tau \right). \quad (10)$$

3.2 Covariance of force part and itself

According to figure 3, we have that $\langle \delta w_f(t_0; \tau_0) \delta w_f(t_0 + \tau; \tau_0) \rangle$

- decays algebraically at low persistence length $l_p/\sigma = 2$,
- decays logarithmically at high persistence length $l_p/\sigma = 20$.

We show the buildup of this covariance with increasing persistence length in figure 4.

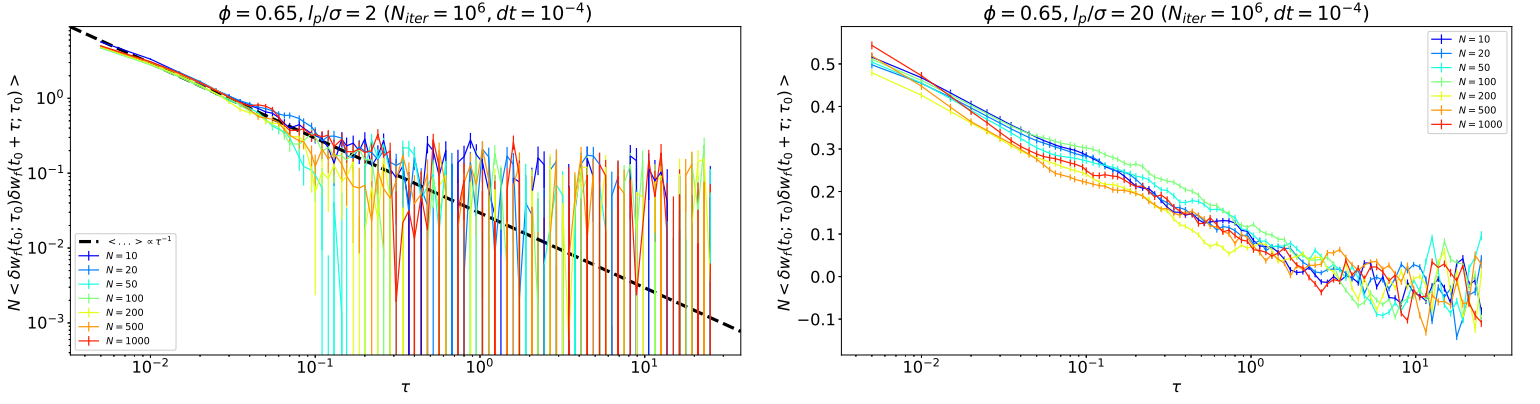


Figure 3: Covariance of the force part of the active work and itself with a delay τ for $l_p/\sigma = 2$ (left) and $l_p/\sigma = 20$ (right).

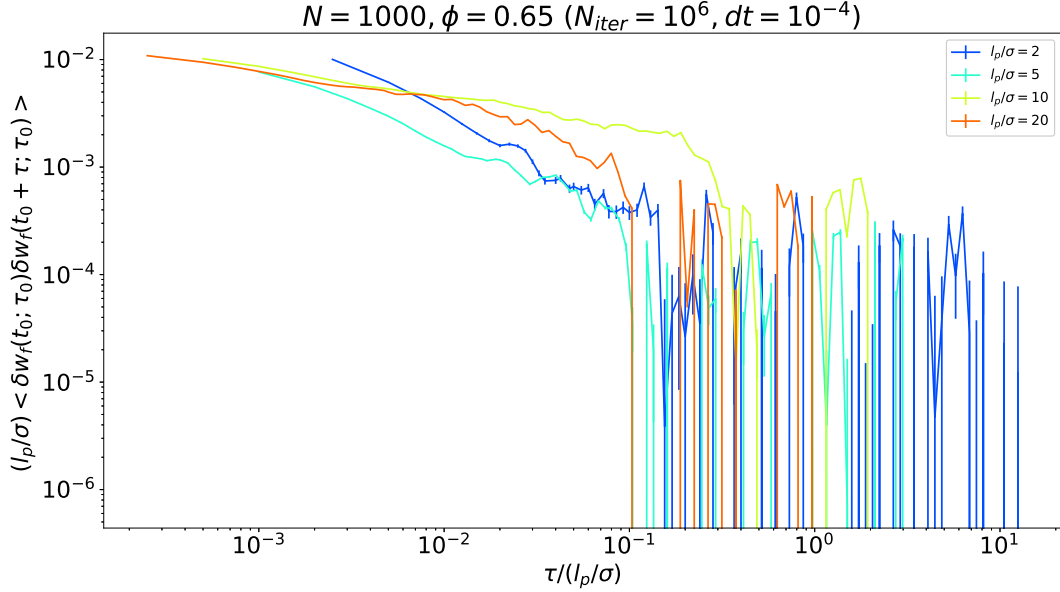


Figure 4: Covariance of the force part of the active work and itself with a delay τ for $2 \leq l_p/\sigma \leq 20$ at $N = 10^3$ particles.

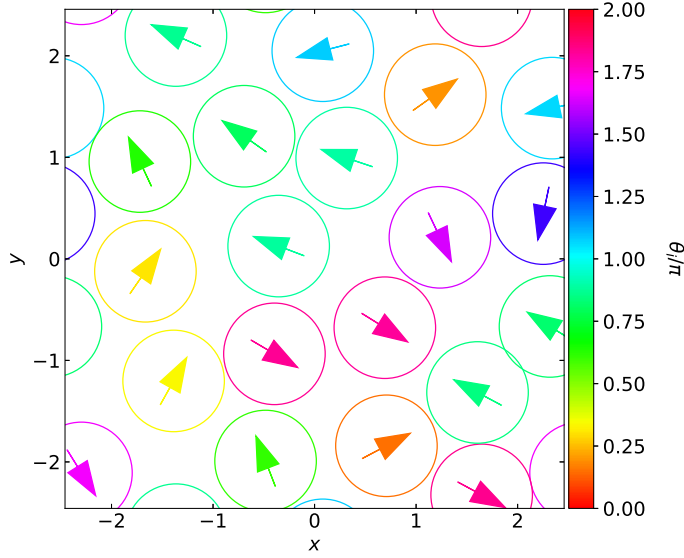
According to [2], the mean force part of the normalised rate of active work in steady state is linked to the structure of the liquid,

$$\langle w_f \rangle = \phi \int g(\underline{r}) \left\{ [\nabla V(\underline{r})]^2 - \frac{2}{3} \frac{\sigma}{l_p} \nabla^2 V(\underline{r}) \right\} d\underline{r} + \phi^2 \iint g_3(\underline{r}, \underline{r}') \nabla V(\underline{r}) \cdot \nabla V(\underline{r}') d\underline{r} d\underline{r}', \quad (11)$$

where g and g_3 are the two- and three-body density correlations among particles.

Maybe then is the decay of $\langle \delta w_f(t_0; \tau_0) \delta w_f(t_0 + \tau; \tau_0) \rangle$ linked to the relaxation of the structure. We have that at $l_p/\sigma = 2$ the system resembles an homogeneous liquid, while at $l_p/\sigma = 20$ denser regions – clusters – appear (figure 5). Moreover, clusters are expected to get denser as the persistence length increases, and particles move more slowly in denser regions [3]. We can thus imagine that the buildup of the covariance of the force part of the active work and itself with a delay τ is directly linked to this changing dynamical picture with increasing persistence length. Such a link remains to be demonstrated.

$N = 2.00e + 01, \phi = 0.65, l_p/\sigma = 2.00e + 00, L = 4.916e + 00$
 $t/(l_p/\sigma) = 2.50000e + 02$



$N = 2.00e + 01, \phi = 0.65, l_p/\sigma = 2.00e + 01, L = 4.916e + 00$
 $t/(l_p/\sigma) = 2.50000e + 01$

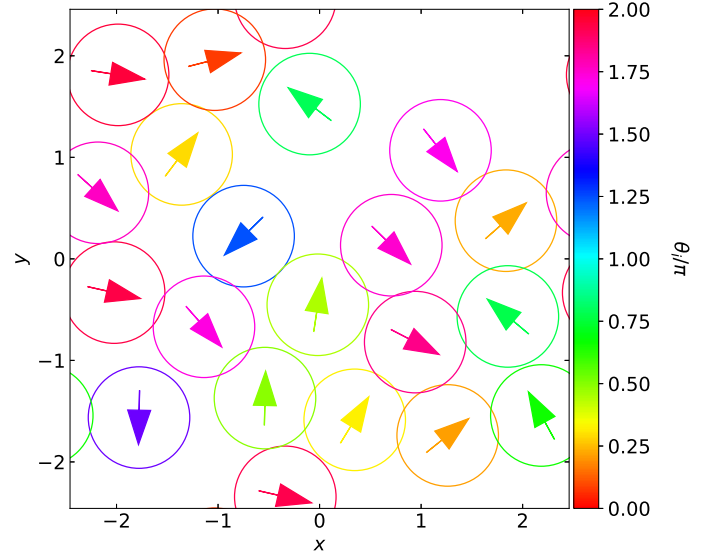


Figure 5: Screenshots of the system for $l_p/\sigma = 2$ (left) and $l_p/\sigma = 20$ (right). Colors refer to the orientation of the particles.

4 Order and active work

We compute the correlation function between the fluctuations of the order parameter norm at time t_0 and the fluctuations of the normalised rate of active work on the interval $[t_0; t_0 + \tau]$ (figure 6),

$$C_{wo}^{(a)}(\tau) = \frac{\langle \delta w(t_0; \tau) \delta |\underline{\nu}(t_0)| \rangle}{\sqrt{\langle \delta w(t_0; \tau)^2 \rangle \langle \delta |\underline{\nu}(t_0)|^2 \rangle}}. \quad (12)$$

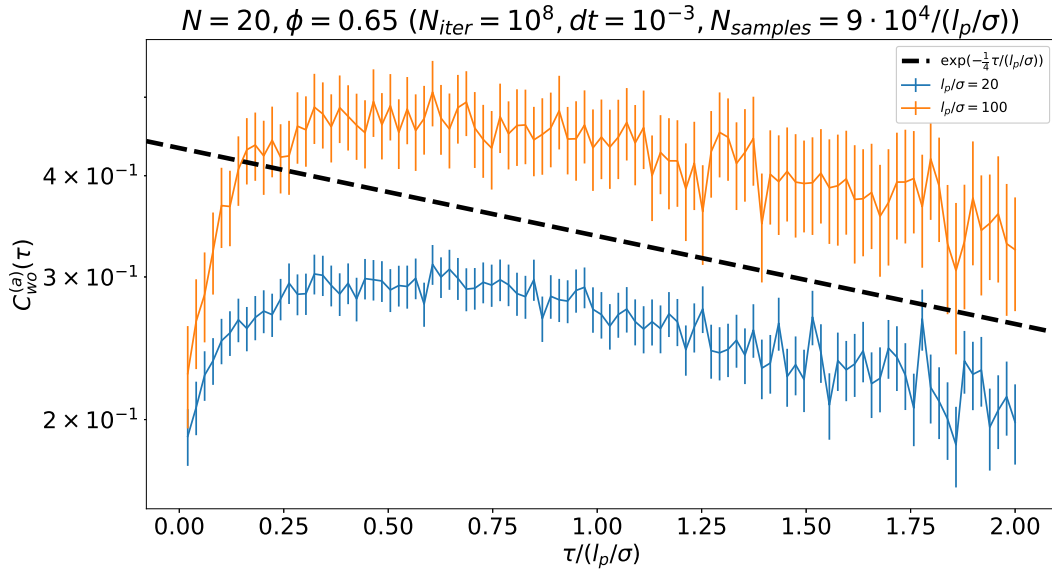


Figure 6: Correlation function between the fluctuations of the order parameter norm at time t_0 and the fluctuations of the normalised rate of active work on the interval $[t_0; t_0 + \tau]$.

First of all, we note that this correlation function is non-monotonic. This can be rationalised by the fact that the variance of the active work,

$$\tau \mapsto \langle \delta w(t_0; \tau)^2 \rangle,$$

is a monotonically decreasing function of τ .

We have that the fluctuations of the normalised rate of active work w over an interval $[t_0; t_0 + \tau]$ are positively correlated with fluctuations of the order parameter $|\underline{\nu}|$ at the beginning of this interval. This may indicate that positive fluctuations of the order parameter norm at a given time leads to an increased active work at following times. This can be explained by the fact that nematically ordered particles – *i.e.* high $|\underline{\nu}|$ – have fewer collisions, so that active forces translates more efficiently into particle motion [1].

We also note that these correlations decay on a length scale larger than the rotational diffusion time – the dashed black line is here for illustration purposes and does not reflect any theoretical prediction. Furthermore, we have that the correlations between the averaged active work and the order parameter norm are higher for $l_p/\sigma = 100$ than for $l_p/\sigma = 20$ – this may however be due, in part or completely, to the fact that the variance of the active work is higher in the latter.

We also compute the covariance of the order parameter norm and the normalised rate of active work with a delay τ (figure 7),

$$\tau \mapsto \langle \delta|\underline{\nu}|(t_0) | \delta w(t_0 + \tau; \tau_0) \rangle, \quad (13)$$

which is linked to the numerator in equation 12 by summation over the interval $[t_0; t_0 + \tau]$.

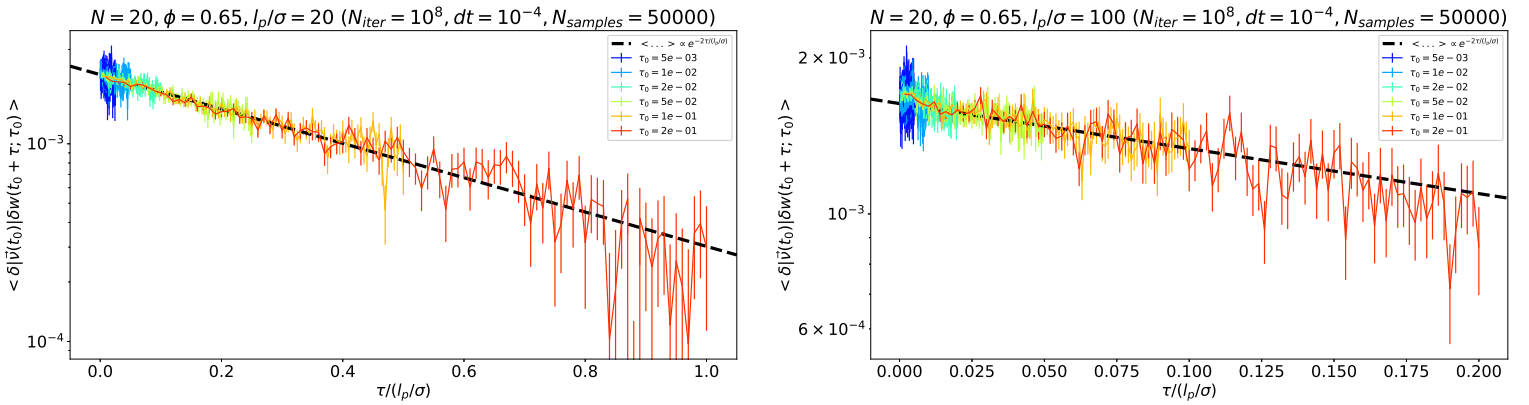


Figure 7: Covariance of the order parameter norm and the normalised rate of active work with a delay τ for $l_p/\sigma = 20$ (left) and $l_p/\sigma = 100$ (right).

We have a monotonic decrease of this covariance with a length scale $\sim \frac{1}{2} \frac{l_p}{\sigma}$ for both tested values of the persistence length.

References

- [1] Takahiro Nemoto, Étienne Fodor, Michael E. Cates, Robert L. Jack, and Julien Tailleur. Optimizing active work: Dynamical phase transitions, collective motion, and jamming. *Physical Review E*, 99(2), February 2019. ISSN 2470-0045, 2470-0053. doi: 10.1103/PhysRevE.99.022605. URL <https://link.aps.org/doi/10.1103/PhysRevE.99.022605>. arXiv:1805.02887 [cond-mat].
- [2] Laura Tociu, Étienne Fodor, Takahiro Nemoto, and Suriyanarayanan Vaikuntanathan. How dissipation constrains fluctuations in nonequilibrium liquids: Diffusion, structure and biased interactions. *arXiv:1808.07838 [cond-mat]*, August 2018. URL <http://arxiv.org/abs/1808.07838>. arXiv: 1808.07838.
- [3] Michael E. Cates and Julien Tailleur. Motility-Induced Phase Separation. *Annual Review of Condensed Matter Physics*, 6 (1):219–244, March 2015. ISSN 1947-5454, 1947-5462. doi: 10.1146/annurev-conmatphys-031214-014710. URL <http://www.annualreviews.org/doi/10.1146/annurev-conmatphys-031214-014710>.